The 2009 IEEE/RSJ International Conference on
Intelligent Robots and Systems
October 11-15, 2009 St. Louis, USA

# Optimal Estimation of Human Body Segments Dynamics Using Realtime Visual Feedback

Gentiane Venture[2], Ko Ayusawa[1], Yoshihiko Nakamura[1]

*Abstract*— **Mass parameters of the human body segments are mandatory when studying motion dynamics. In orthopedics, biomechanics and rehabilitation they are of crucial importance. Inaccuracies their value generate errors in the motion analysis, misleading the interpretation of results. No systematic method to estimate them has been proposed so far. Rather, parameters are scaled from generic tables or estimated with methods inappropriate for in-patient care. Based on our previous works, we propose a real-time software and its interface that allow to estimate the whole-body segment parameters, and to visualize the progresses of the completion of the identification. The visualization is used as a visual feedback to optimize the excitation and thus the identification results. The method is experimentally tested and obtained results are discussed.**

## I. Introduction

The appropriate knowledge of segment parameters is of crucial importance when one studies the human motions dynamics. With an accurate knowledge of the subject specific segment parameter is is possible to refine diagnosis and personalize health-care; on the contrary it is shown in [1] that errors in the body-segment mass-parameter affect significantly the analysis results. In orthopedics, biomechanics, neurology, musculoskeletal disorders studies is an important information, it allows to monitor directly the parameters, and also to compute the position of the whole body center of mass (COM). Its trajectory is often use in gait studies; the computation of the segment parameters (SP): inertia and the position of the COM of each link, is a key-step in gait analysis and to monitor the variations of muscle mass due to disease, hospitalization, rehabilitation or training [2]. Systems to estimate in-vivo the position of the whole-body COM have been recently released thanks to the developments in portable technologies [3], [4]. Nevertheless, the inertias are usually not estimated in-vivo, by lack of accurate methodologies, and are computed by interpolations of literature data [5], [6]. These data are obtained by photogrammetry [7], known to be poorly accurate, or more recently by 3D imaging (CT-scan or MRI) and 3D modeling interpolations, known to be expensive (equipment and time) and hazardous (radiations) [8], [9]. Discrepancies in body landmarks and in models of the human-body [10] as well as the profusion of references make an adequate choice difficult. In addition, proper interpolations of the available data require hundreds of geometric measurements which are often inaccurate. Consequently, there is a urge of reliable and robust methods to estimate in-vivo the SP of the human body.

Based on our previous works on identification of human-body base-parameters [11], we present in this paper a methodology to perform real-time estimation of the whole-body SP. The required measurements are motion and contact force [12]. We have also developed a graphic interface that is used to generate optimal exciting trajectories from visual feedback thanks to which we obtain more accurate results in a shorter time. This method allows in-vivo subject-specific identification of the SP with a fast, safe and robust environment. It makes use of both the identification of the base-parameters and an interpolation from the data-base of the human body dynamics [13].

## II. Base parameters identification from contact forces and motion data

### A. General identification model of legged systems

From [14], [15] and [16], [17], the inverse dynamics is written in a linear form with respect to the SP as shown in [11]. And by separating the vector of constant inertial parameters, we obtain the identification model Eq. 1.

$$\boldsymbol{Y}\boldsymbol{\phi} = \begin{bmatrix}\boldsymbol{Y}_O \\ \boldsymbol{Y}_C\end{bmatrix}\boldsymbol{\phi} = \begin{bmatrix}\boldsymbol{0} \\ \boldsymbol{\tau}\end{bmatrix} + \sum_{k=1}^{N_c}\begin{bmatrix}\boldsymbol{J}_{Ok}^T \\ \boldsymbol{J}_{Ck}^T\end{bmatrix}\boldsymbol{F}_k^{ext} \qquad (1)$$

where:

- $\boldsymbol{\tau} \in \boldsymbol{R}^{N_J-6}$ is the vector of joint torques,
- $N_c$ is the number of contact points with the environment,
- $\boldsymbol{F}_k^{ext} \in \boldsymbol{R}^6$ is the vector of external forces exerted to the humanoid at contact $k$,
- $\boldsymbol{J}_k = [\boldsymbol{J}_{Ok}\ \boldsymbol{J}_{Ck}] \in \boldsymbol{R}^{6\times N_J}$ are the basic Jacobian matrices of the position at contact $k$ and of the orientation of the contact link with respect to $\boldsymbol{q_0}$ and $\boldsymbol{q_c}$, which are used to map $\boldsymbol{F}_k^{ext}$ to the vector of generalized forces.
- $\boldsymbol{\phi} \in \boldsymbol{R}^{10n}$ is the vector of segment parameters (SP).
- $\boldsymbol{Y} = \begin{bmatrix}\boldsymbol{Y}_O \\ \boldsymbol{Y}_C\end{bmatrix} \in \boldsymbol{R}^{N_J\times 10n}$ is the regressor, a function matrix of generalized coordinates $\boldsymbol{q_0}$ of the base-link, the joint angles $\boldsymbol{q_c}$, and their derivatives $\dot{\boldsymbol{q}}_0$, $\dot{\boldsymbol{q}}_c$, $\ddot{\boldsymbol{q}}_0$, $\ddot{\boldsymbol{q}}_c$. $\boldsymbol{Y}_O \in \boldsymbol{R}^{6\times 10n}$ is the regressor corresponding in the six equations of motion of the base-link.

Only the minimal set of inertial parameters that describes the dynamics of the system can be identified. This set is called base parameters $\boldsymbol{\phi}_B \in \boldsymbol{R}^{N_B}$. It can be computed symbolically or numerically from the vector of SP $\boldsymbol{\phi}$ by

This research is supported by the Special Coordination Funds for Promoting Science and Technology: "IRT Foundation to Support Man and Aging Society". And by Category S of Grant-in-Aid for Scientific Research (20220001), Japan Society for the Promotion of Science.

[1] Department of Mechano-Informatics, The University of Tokyo, Japan
[2] Department of Mechanical System Engineering, The Tokyo University of Agriculture and Technology, Japan venture@cc.tuat.ac.jp

eliminating those that have no influence on the model and regrouping some according to the kinematics of the system [18]–[20]. The base parameters $\boldsymbol{\phi}_B \in \boldsymbol{R}^{N_B}$ can be calculated symbolically from the standard parameters $\boldsymbol{\phi} \in \boldsymbol{R}^{10n}$ as follows:

$$\boldsymbol{\phi}_B = \boldsymbol{Z}\boldsymbol{\phi} \tag{2}$$

Where, $\boldsymbol{Z} \in \boldsymbol{R}^{N_B \times 10n}$ is the composition matrix of base parameters [21].

We obtain the minimal identification model given by Eq. 3. $\boldsymbol{Y}_B \in \boldsymbol{R}^{N_J \times N_B}$ is called the regressor for the base parameters and is of full-rank.

$$\boldsymbol{Y}_B\boldsymbol{\phi}_B = \begin{bmatrix} \boldsymbol{Y}_{OB} \\ \boldsymbol{Y}_{CB} \end{bmatrix} \boldsymbol{\phi}_B = \begin{bmatrix} \boldsymbol{0} \\ \boldsymbol{\tau} \end{bmatrix} + \sum_{k=1}^{N_c} \begin{bmatrix} \boldsymbol{J}_{Ok}^T \\ \boldsymbol{J}_{Ck}^T \end{bmatrix} \boldsymbol{F}_k^{ext} \tag{3}$$

### *B. Identification model from base-link dynamics*

Most identification methods are based on solving Eq. 3, consequently they require the measurement of:

- the base-link information $\boldsymbol{q}_0$,
- the chains information $\boldsymbol{q}_c$ and $\boldsymbol{\tau}$,
- the external forces $\boldsymbol{F}_k^{ext}$ for the $N_c$ contact points.

However it is difficult to measure accurately $\boldsymbol{\tau}$ as this is a function of the muscle forces and the joint visco-elastic characteristics of the joint. In [11] we proposed to identify $\boldsymbol{\phi}_B$ using only the upper-part of the identification model Eq. 3: the equations of motion of the base-link, and thus to estimate the pure SP.

$$\boldsymbol{Y}_{OB}\boldsymbol{\phi}_B = \sum_{k=1}^{N_c} \boldsymbol{J}_{Ok}^T \boldsymbol{F}_k^{ext} \tag{4}$$

We obtain a system given by Eq. 4 that is not function of the joint torque $\boldsymbol{\tau}$. Consequently to estimate the set of base parameters $\boldsymbol{\phi}_B$, the measurement of the joint torques is not required. Solely the measurement of the $k$ contact forces $\boldsymbol{F}_k^{ext}$, the joint angles $\boldsymbol{q}_c$ and the generalized coordinates $\boldsymbol{q}_0$ are required. This information is measured by motion capture and force-plates. As we directly measure the contact forces $\boldsymbol{F}^{ext}$ it is not necessary to discriminate the support phases.

However, this method stands only if the reduction of the system to these six equations keeps unchanged the number of parameters that are structurally identifiable. This has been demonstrated mathematically in [21]; thus the structural identifiability of the base parameters is maintained and Eq. 4 leads to similarly identify the whole set of base parameters.

The estimate of the vector of base parameters $\hat{\boldsymbol{\phi}}_B$ is obtained by solving Eq. 4 with the least square method, or the weighted least square method. This correspond in minimizing the optimal criterion given by Eq.5

$$\min_{\boldsymbol{\phi}_B} \| \sum_{k=1}^{N_c} \boldsymbol{J}_{Ok}^T \boldsymbol{F}_k^{ext} - \boldsymbol{Y}_{OB}\boldsymbol{\phi}_B \|^2 \tag{5}$$

## III. Estimation of whole-body SP

The base parameters $\boldsymbol{\phi}_B$ are the necessary and sufficient information to compute the equations of motion, thus the only parameters identifiable straightforwardly from Eq. 3 and Eq. 4. They are obtained by eliminating and regrouping the standard parameters $\boldsymbol{\phi}$ according to the kinematics [12], so they are too complicated terms to be comprehended naturally and to provide a sufficient physiological meaning. Therefore, for medical applications the standard SP $\boldsymbol{\phi}$ are more comprehensible than the base parameters $\boldsymbol{\phi}_B$.

After identification of the base parameters $\hat{\boldsymbol{\phi}}_B$ as shown in section II-B it is possible to compute the standard parameters $\boldsymbol{\phi}$ by projecting the identified base-parameters in the standard-parameters space and extrapolating the missing information from literature data or data-base, to obtain finally the whole set of SP with certainty. The estimated standard parameters meet the base-parameters without distortion, and minimize the error of information from data-base for the standard parameters.

For the linear equation (2), the general form of the least-squares solution for a rank-deficient regressor is given by [22]:

$$\boldsymbol{\phi} = \boldsymbol{Z}^{\#}\phi_B + (\boldsymbol{E} - \boldsymbol{Z}^{\#}\boldsymbol{Z})\boldsymbol{z} \tag{6}$$

where $\boldsymbol{z} \in \boldsymbol{R}^{10n}$ is an arbitrary vector, and $\boldsymbol{E}$ is the identity matrix. When using the identified base parameters $\hat{\boldsymbol{\phi}}_B$, the main problem resides in determining the vector $\boldsymbol{z}$ projected to the null space of the composition matrix $\boldsymbol{Z}$

We choose the vector $\boldsymbol{z} = \boldsymbol{\phi}^{ref}$, where $\boldsymbol{\phi}^{ref}$ is the information found in the data-base for the standard parameters or reference standard parameters, and finally the subject-specific standard parameters $\hat{\boldsymbol{\phi}}$ can be obtained as follow:

$$\begin{aligned} \hat{\boldsymbol{\phi}} &= \boldsymbol{Z}^{\#}\hat{\boldsymbol{\phi}}_B + (\boldsymbol{E} - \boldsymbol{Z}^{\#}\boldsymbol{Z})\boldsymbol{\phi}^{ref} \\ &= \boldsymbol{\phi}^{ref} + \boldsymbol{Z}^{\#}(\hat{\boldsymbol{\phi}}_B - {\boldsymbol{\phi}_B}^{ref}) \end{aligned} \tag{7}$$

Where, ${\boldsymbol{\phi}_B}^{ref} = \boldsymbol{Z}\boldsymbol{\phi}^{ref}$.

Eq. 7 satisfies Eq. 2. Eq. 7 also implies that $\hat{\boldsymbol{\phi}}$ minimizes $||\boldsymbol{\phi} - \boldsymbol{\phi}^{ref}||$, which means the error of the reference standard parameters $\boldsymbol{\phi}^{ref}$.

## IV. Real-time visualization of identification results

We present the outline of the application to visualize the identification result using the real-time identification method. Each step is then detailed in the following subsections. The human motions are recorded every 5[ms] by a commercial optical motion capture system consisting in 10 cameras (Motion Analysis) and 35 reflective optical markers, and the contact forces are measured every 1[ms] by the force-plates (Kistler). The model of human consists in 34 degrees of freedom [11]. The motion-data and the force-data are synchronized. The identification process is as follows (Fig. 1):

1) the geometric model of human is defined, measure the geometric parameters of the model from motion capture, and estimate the prior standard inertial parameters from geometric parameters and the data-base.

2) From the motion capture and force-plates, we identify the base parameters and the standard parameters using the real-time method.
3) Using colored presentation to specify the links yet not to be identified, we can improve the quality of identification results.

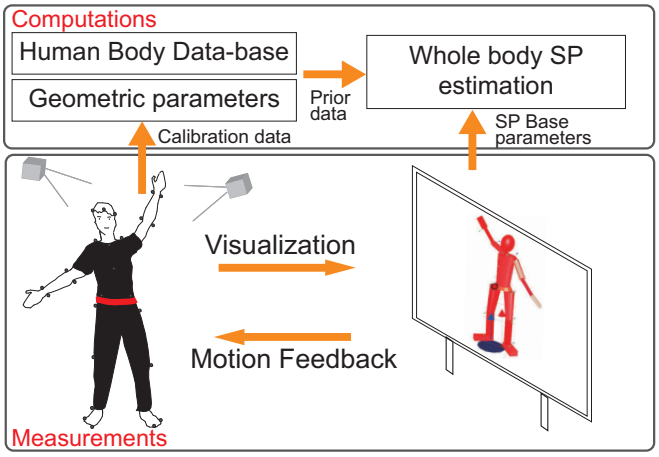


Fig. 1. Conceptual diagram of the proposed approach of real-time identification and visualization

### A. Estimation of the geometric model and initial estimation of standard inertial parameters

To obtain good results it is important to define the kinematic model used to describe the human body, and to obtain its characteristic geometric parameters. As discussed in our previous work, the modeling depends on the purpose of identification and the real constraints such as the measurement facility [11]. We consider a model of the human body consisting in 34 DOF and 15 rigid links as follows: the waist, the neck, the shoulders, the wrists, the hip joints and the ankles are modeled with spherical joints. The elbows and the knees are modeled with rotational joints. They represent the most important DOF that are used in daily activities such as locomotion. DOF can be added and removed according to the needs, keeping in mind that a compromise is necessary between the number of DOF and the identifiability (smallness, excitation) of the SP.

Geometric parameters are by nature measurable directly. Usually they are measured manually, here we propose to use an automatic method making use of the defined positions of the optical markers. They are located at the defined anatomical points to insure the accuracy when computing the inverse kinematics, thus we can automatically compute the geometric parameters of each link by calculating the relative position of the markers.

The standard inertial parameters (reference) are then estimated from the obtained geometric model, in order to build the model shape. In this paper, we apply the method described in [13] and that makes use of the data-base of the human body available from [23], to estimate the standard inertial parameters of the human body. The data-base consists in the 49 diagnostic measurements and the total body mass of 308 Japanese. The initial estimation of the standard parameters is performed as follows:

1) We automatically measure 49 diagnostic measurements and the total mass (from marker positions and force-plates data) to use as inputs of the initial estimation routine to compute the other items using a linear regression.
2) The geometric shape of the human body is modeled by simple primitive shapes. For example, oval sphere, truncated cone, and boxes as shown in Fig. 2.
3) The size and volume of each primitive is computed from the 49 measurement items, and the inertial parameters are obtained, assuming that the density of each link is uniform.

An example is given in Fig. 2 for 3 male subjects of different morphologies. From left to right the body height and weight are: $1.73m$ $58Kg$, $1.62m$ $54Kg$ and $1.76m$ $76.3Kg$. The differences in body shape are clearly visible from the obtained model shapes.

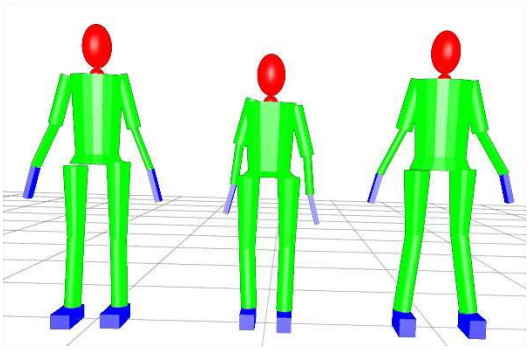

Fig. 2. The geometrically approximate shape of human in 3 different cases: from left to right the body height and weight are: $1.73m$ $58Kg$, $1.62m$ $54Kg$ and $1.76m$ $76.3Kg$

### B. Real-time implementation of the identification of the base parameters

From the inverse kinematics computations of marker positions, the generalized coordinates and their derivatives are obtained, and the regressor in Eq. 4 is calculated in real-time. The total external force exerted to the frame of the base-link is calculated from the force-plates data using Eq. 4.

For real-time computation, the on-line least squares algorithm is implemented, however with this method an initial value for $\phi_{B0}$ is necessary. Actually, the forces and moments of the 6-axis external force in Eq. 4 have different physical units, and different measurement accuracies. To avoid discrepancies in the results the weighted least squares method is used, attributing a different weight to the 6 components. In addition, some parameters may be time-varying, for example when a human handles or releases an object during the measurements, to identify appropriately the parameters an exponential forgetting coefficient $\lambda_n$ is used [24]. The above features are implemented as follow: At times $t = [1 \cdots n]$, the estimated parameters $\phi_{B,n}$ at $t = n$ is computed from

$\boldsymbol{\phi}_{B,n-1}$ at $t = n-1$ as follow.

$$\hat{\boldsymbol{\phi}}_{B,n} = \lambda_n \hat{\boldsymbol{\phi}}_{B,n-1} + \boldsymbol{K}_n(\boldsymbol{F}_n - \boldsymbol{Y}_{OB,n}\hat{\boldsymbol{\phi}}_{B,n-1}) \quad (8)$$

Where,

- $\lambda_n (0 \leq \lambda_n \leq 1)$ is the time-varying forgetting factor.
- $\boldsymbol{Y}_{OB,n}$ and $\boldsymbol{F}_n$ are the regressor and the external force in Eq. 4 at the time $t = n$.
- $\boldsymbol{K}_n \in \boldsymbol{R}^{N_B \times N_B}$ is the gain matrix as follow:

$$\boldsymbol{K}_n = \boldsymbol{P}_{n-1}{\boldsymbol{Y}_{OB,n}}^T {\boldsymbol{V}_n}^{-1} \quad (9)$$

- $\boldsymbol{V}_n \in \boldsymbol{R}^{6\times 6}$ is defined as follow:

$$\boldsymbol{V}_n = \lambda_n \boldsymbol{\Sigma_n} + \boldsymbol{Y}_{w,t}\boldsymbol{P}_{n-1}{\boldsymbol{Y}_{w,t}}^T \quad (10)$$

- $\boldsymbol{P}_n \in \boldsymbol{R}^{N_B \times N_B}$ is defined by defined by:

$$\boldsymbol{P}_n = \sum_{n=i}^{n} ({\boldsymbol{Y}_{OB,i}}^T \boldsymbol{\Sigma}_i \boldsymbol{Y}_{OB,i})^{-1} \quad (11)$$

And the on-line inverse matrix calculation is given by:

$$\boldsymbol{P}_n = \frac{1}{\lambda_n}(\boldsymbol{P}_{n-1} - \boldsymbol{P}_{n-1}{\boldsymbol{Y}_{OB,n}}^T {\boldsymbol{V}_n}^{-1}\boldsymbol{Y}_{OB,n}\boldsymbol{P}_{n-1}) \quad (12)$$

- $\boldsymbol{\Sigma_n} \in \boldsymbol{R}^{6\times 6}$ is the weighted matrix.

The weighted matrix $\boldsymbol{\Sigma}_n$ is chosen as the covariance matrix for the disturbance of $\boldsymbol{F}$. We consider that the 6 axis elements of $\boldsymbol{F}$ are independent and thus $\boldsymbol{\Sigma}_n$ is diagonal. The i-th diagonal element $\sigma^2_{ii,n} (1 \leq i \leq 6)$ is the variance of the estimated error of each component of $\boldsymbol{F}$. $\sigma_{ii,n}$ can be calculated using $\boldsymbol{A}_{i,n} \in \boldsymbol{R}^{N_B \times N_B}$, $\boldsymbol{b}_{i,n} \in \boldsymbol{R}^{N_B}$, $c_{i,n} \in \boldsymbol{R}$, $d_n \in \boldsymbol{R}$ as follow, where $f_{i,n} \in \boldsymbol{R}$, $\boldsymbol{y}_{i,n} \in \boldsymbol{R}^{1\times N_B} (1 \leq i \leq 6)$ are the each component of respectively $\boldsymbol{F}_n$ and $\boldsymbol{Y}_{OB,n}$.

$${\sigma_{i,n}}^2 = \frac{1}{d_n}({\boldsymbol{\phi}_{B,n-1}}^T \boldsymbol{A}_{i,n}\boldsymbol{\phi}_{B,n-1} - 2{\boldsymbol{\phi}_{B,n}}^T \boldsymbol{b}_{i,n} + c_{i,n}) \quad (13)$$

$$\boldsymbol{A}_{i,n} = {\boldsymbol{y}_{i,n}}^T \boldsymbol{y}_{i,n} + \lambda_n^2 \boldsymbol{A}_{i,n-1} \quad (14)$$

$$\boldsymbol{b}_{i,n} = f_{i,n}{\boldsymbol{y}_{i,n}}^T + \lambda_n^2 \boldsymbol{b}_{i,n-1} \quad (15)$$

$$c_{i,n} = {f_{i,n}}^2 + \lambda_n^2 c_{i,n-1} \quad (16)$$

$$d_n = 1 + \lambda_n d_{n-1} \quad (17)$$

From Eq. 8, Eq. 12, and Eq. 13 - (17), we can compute $\boldsymbol{V}_n$, $\boldsymbol{P}_n$, and $\hat{\boldsymbol{\phi}}_{B,n}$ every time, and also obtain $\hat{\boldsymbol{\phi}}_n$ from Eq. 7. The initial value for $\boldsymbol{P}_0$, $\hat{\boldsymbol{\phi}}_{B0}$ and $\hat{\boldsymbol{\phi}}_0$ can be chosen as a-priori knowledge. If they are unknown, we choose $\hat{\boldsymbol{\phi}}_{B0} = \boldsymbol{0}$, $\hat{\boldsymbol{\phi}}_0 = \boldsymbol{0}$ and $\boldsymbol{P}_0 = \gamma \boldsymbol{E}$. Similarly, $\boldsymbol{A}_{i,0}, \boldsymbol{b}_{i,0}, c_{i,0}, d_{i,0}$ are chosen as zeros without a-priori data. A large value of $\gamma (> 0)$ leads to a fast convergence of the identification procedure, nevertheless $\boldsymbol{P}_n$ becomes unstable with lack of exciting motion data. The forgetting factor $\lambda_n$ is often chosen with a constant value from 0.995 to 1. If the parameters are constant (no object carried) $\lambda = 1$ is chosen (no forgetting); if the parameters are to change (when handling and releasing objects) we chose $\lambda < 1$.

## V. Optimal Exciting Trajectories

The accuracy of the identified base parameters highly depends in the motion used to sample the identification model. It is important to sample the identification model along a motion that excites the system dynamics to be estimated. Such motions are called Persistent Exciting Trajectories [25]. A criterion to define an appropriate motion is to consider motion leading to small value of the condition number of the obtained regressor. However, a large number of DOF and time-varying contact situation complicate the definition of persistent exciting trajectories [26]. In addition optimal exciting trajectories guaranty the robustness of the on-line least square convergence with respect to the initial parameters $\boldsymbol{\phi}_{B0}$.

We make use of the real-time identification to visualize the identification as well as adjust the persistent exciting movements. During the measurement, we display the model using a colored representation for the identified link parameters and the not yet identified link parameters. It allows to intuitively recognize which links need to be excited. The examinee gets the feedback from the display and can generate the adequate persistent exciting trajectories in order to improve the identification results. the colors are chosen according to the relative standard deviation calculated for each base parameter. In fact, he relative standard deviations computed for each parameter [25], [27] are a statistical indicator of the identification results quality. Considering that the regressor $\boldsymbol{Y}_{OB}$ of the linear system Eq. 4 is a deterministic one, and the modeling error $\boldsymbol{\rho} = \boldsymbol{F} - \boldsymbol{Y}_{OB}\hat{\boldsymbol{\phi}}_B$ is a zero mean Gaussian noise, the covariance matrix $\boldsymbol{C}_n \in \boldsymbol{R}^{N_B \times N_B}$ of the estimation error of $\hat{\boldsymbol{\phi}}_{B,n}$ are computed as follow:

$$\boldsymbol{C}_n = E((\boldsymbol{\phi}_B - \hat{\boldsymbol{\phi}}_{B,n})(\boldsymbol{\phi}_B - \hat{\boldsymbol{\phi}}_{B,n})^T) = \boldsymbol{P}_n \quad (18)$$

where E is the expectation operator. Eq. 8, Eq. 9, and Eq. 12 of the on-line least squares algorithm are similar to equations of a Kalman filter without the system noise , and $\boldsymbol{P}_n$ is equivalent to the covariance matrix of $\boldsymbol{C}_n$.

$c_{n,(i,i)}$ is the diagonal elements of $\boldsymbol{C}_n$, and the relative standard deviation $\sigma_{\phi_j\%}$ is thus computed as follow:

$$\sigma_{\phi_j,n\%} = 100\frac{\sqrt{c_{n,(i,i)}}}{\hat{\phi}_{Bj,n}} \quad (19)$$

We consider that a parameter with a relative standard deviation $\sigma_{\phi_j\%}$ lower than a specified threshold is well identified, keeping in mind that this is only an indicator based on statistical assumptions. However for parameters with small values, they may be well identified although $\sigma_{\phi_j\%}$ is large.

The results are visualized in an active interface using the 3D representation of the human figure defined in section IV-A. The color of each link is adjusted in real-time and defined according to a simple rule as follow: $n_{Bj}$ is the number of the base parameters of the link $j$, $n_{Bj,G}$ is the number of parameters that $\sigma_{\phi_j\%}$ is lower than 10[%], $n_{Bj,B}$ is the number of parameters that $\sigma_{\phi_j\%}$ is not lower than 10[%] but small parameters($< 0.02$), and $n_{Bj,R} = n_{Bj} - n_{Bj,G} -$

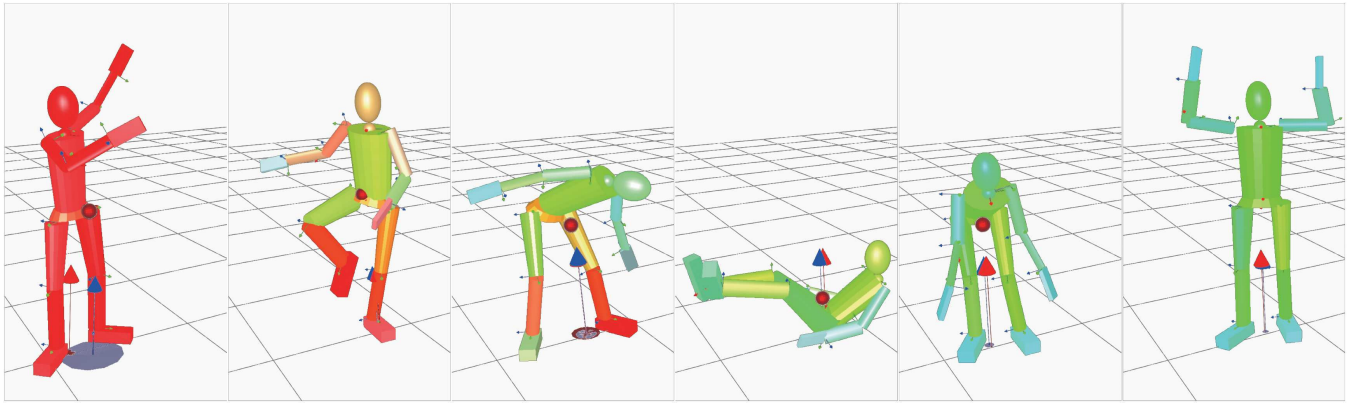

Fig. 3. Real-time identification of human inertial parameters

$n_{Bj,B}$. Then rgb color values of each link are chosen as ratio of $n_{Bj,R}$, $n_{Bj,G}$, and $n_{Bj,B}$. Starting from red for non identified parameters to green for fully identified parameters; and cyan for small parameters, as can be seen in Fig. 3.

## VI. Experiments

We compare the results obtained with the standard off-line identification procedure and the optimal identification procedure featuring the visual feed back. For that we record motions that are known to be persistent exciting trajectories and have proven to allow identifying the whole body base-parameters [26]. In addition we record three motions using the real-time visualization interface. During this phase the motions are free and only adjusted to provided the identification of the parameters based on the color changes. The initial conditions for real-time identification are $\lambda_n = 1.0$, $\gamma = 0.001$, and other parameters are zeros.

### A. Identification of base parameters

The identification results of the base-parameters obtained for 3 motions are given in Table I. The condition number or the regressor $\mathrm{cond}(\boldsymbol{Y}_{OB})$ and the length of data-set of each motion are presented. The number of estimated parameters $n_{est} = n_{Bj,G} + n_{Bj,B}$ is also shown. Usually randomly chosen motions of the whole body lead to regressor of high condition number about 500. Using the combination of several motions from a gymnastic TV program has lead to condition number about 40 [26]. Table I shows that when using the interface lead to obtain condition numbers of about 30. And thus to enhance the excitation properties of the recorded motions by visual feedback and the quality of the estimation. more particularly for the extremities of the limb and the head.

TABLE I

Summary of experimental identification results (base parameters)

| Motion ID | 1 | 2 | 3 | all |
|---|---|---|---|---|
| $\boldsymbol{Y}_B$ | 35.8 | 30.8 | 23.3 | 25.3 |
| length of data-set | 2660 | 4291 | 4007 | 10958 |
| estimated base parameters | 106 | 105 | 110 | 122 |

### B. Identification of standard parameters

The results of the estimation of the standard parameters $\hat{\phi}$ and the initial standard parameters $\phi^{ref}$ are given in Table II. It shows the mass $M$[kg], the center of mass $C_i$[kg-m], and the inertias $J_{ij}$[kg-m$^2$] of 6 links: the lower torso(L1), the upper torso(L2), the right foot(L3), the right hand(L4),the head(L5) and the left thigh(L6).

TABLE II

Estimated standard inertial parameters and literature parameters ($_L$) of six links

| Link | L1 | L2 | L3 | L4 | L5 | L6 |
|---|---|---|---|---|---|---|
| M | 2.79 | 19.38 | 1.94 | 0.43 | 3.91 | 6.01 |
| $M_L$ | 2.51 | 19.08 | 2.50 | 0.48 | 4.03 | 5.73 |
| Cx | -0.04 | -0.03 | -0.03 | -0.01 | -0.05 | 0.08 |
| $Cx_L$ | 0.00 | 0.00 | 0.04 | 0.10 | 0.00 | 0.20 |
| Cy | 0.01 | -0.01 | 0.02 | -0.01 | -0.12 | -0.02 |
| $Cy_L$ | 0.00 | 0.01 | 0.10 | 0.00 | 0.00 | -0.02 |
| Cz | 0.01 | 0.21 | -0.03 | -0.06 | 0.40 | 0.02 |
| $Cz_L$ | 0.03 | 0.23 | 0.00 | 0.00 | 0.16 | 0.00 |
| Jxx | 0.46 | 0.62 | 0.02 | 0.01 | 0.32 | 0.04 |
| $Jxx_L$ | 0.02 | 1.38 | 0.04 | 0.00 | 0.12 | 0.01 |
| Jyy | 0.03 | 0.71 | 0.03 | 0.01 | 0.01 | -0.08 |
| $Jyy_L$ | 0.01 | 1.33 | 0.01 | 0.01 | 0.12 | 0.08 |
| Jzz | -0.01 | 0.01 | 0.07 | 0.01 | -0.09 | -0.15 |
| $Jzz_L$ | 0.02 | 0.14 | 0.05 | 0.01 | 0.01 | 0.09 |

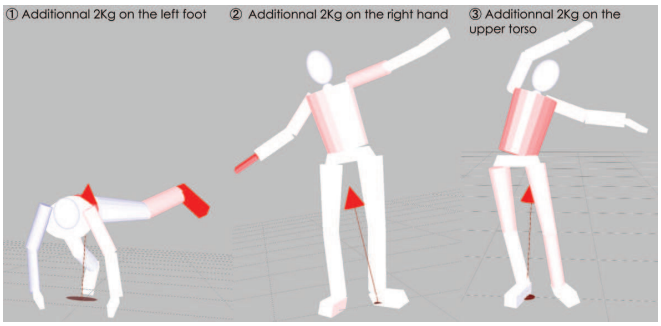


Fig. 4. Monitoring of changes: a 2Kg mass is consecutively added to the left foot, the right hand and the upper-torso

The estimated masses are close to the prior parameters, and the inertias of $L2$, $L3$, $L4$ also shows good correlations. However, the center of mass of $L1$ and $L5$, and the inertia around the Z-axis of $L1$,$L5$ and $L6$ have failed to be estimated, i.e. the center of mass is located outside of the link and the principal moment of inertia around Z-axis is negative. This can be explained as follow: some base parameters of $L1$ and $L6$ have a standard deviation higher than 15%. In addition, the prior standard parameters are not accurate and the data-base is not complete, which affects the estimated standard parameters. We have to improve the accuracy of the presumption of prior information. To solve accurately Eq. 2, the dynamics constraints are to be considered: for example, the center of mass is located inside of the link and the principal moment of inertia must be positive. In order to validate the results and verify the possibility to track time-changing parameters we attached a 2Kg mass at different locations on the body (left foot, right hand, upper torso) and identify the new base-parameters. We use the parameters with no mass as a reference, and then use a colored visualization of the newly identified parameters: the link is proportionally colored in red with the increase in mass and inertia. And in blue with the decrease. Fig. 4 shows the results for the 3 different location of the 2Kg mass.

## VII. Conclusion

We have proposed an identification method for the whole body segment parameters of humans. We have shown that:

- It is possible to estimate all the standard inertial parameters. The proposed method makes use of 1. the identification of the base parameters and 2. the prior estimated parameters extracted from the data-base of human body. The estimated parameters meet the identification results without distortion, and minimize the error of the prior information from data-base.
- The proposed approach of real-time identification and visualization of identification results during measurement allows to generate optimal persistent exciting trajectories, thus to obtain more accurate results with less data.

Further work will consist in developing the constrained algorithm so that all the standard parameters will be physiologically correct. Applications of the method include interfaces for health monitoring and rehabilitation monitoring, as well as tools for gait analysis and orthopedics.

## References


[1] D.J. Pearsall and P.A. Costigan, "The effect of segment parameter error on gait analysis results," *Gait and Posture*, vol. 9, pp. 173–183, 1999.

[2] C.L. Vaughan, J.C. O'Connor, and B.L. Davis, *Dynamics of human gait*, Human Kinetics Publishers, 1992.

[3] A.L. Betker, T. Szturm, and Z. Moussavi, "Center of mass approximation during walking as a function of trunk and swing leg acceleration," in *Proc. of the 28th IEEE EMBS Annual Int. Conf., New York City, USA*, 2006, pp. 3435–3438.

[4] J. Han, A.L. Betker, T. Szturm, and Z. Moussavi, "Estimation of the center of body mass during forward stepping using body aceleration," in *Proc. of the 28th IEEE EMBS Annual Int. Conf., New York City, USA*, 2006, pp. 4564–4567.

[5] J.W. Young, R.F. Chandler, and C.C. Snow, "Anthropometric and mass distribution characteristics of the adult female," Tech. Rep. FAA-AM-83-16, US Air Force, 1983.

[6] J. Durkin and J. Dowling, "Analysis of body segment parameter differences between four human populations and the estimation errors of four popular mathematical models," *J. of Biomedical Eng.*, vol. 125, pp. 515–522, 2003.

[7] R.K. Jensen, "Estimation of the biomechanical properties of three body types using a photogrammetric method," *J.Biomechanics*, vol. 11, pp. 349–358, 1978.

[8] D.J. Pearsall and J.G. Reid, "Inertial properties of the human trunk of males determined from magnetic resonance imaging," *Annals of Biomedical Engineering*, vol. 22, pp. 692–706, 1994.

[9] C.K. Cheng, "Segment inertial properties of chinese adults determined from magnetic resonance imaging," *Clinical biomechanics*, vol. 15, pp. 559–566, 2000.

[10] P. de Leva, "Adjustments to zatsiorsky-seluyanov's segment inertia parameters," *J.of Biomechanics*, vol. 29, no. 9, pp. 1223–1230, 1996.

[11] G. Venture, K. Ayusawa, and Y. Nakamura, "Motion capture based identification of human inertial parameters," in *Proc. IEEE/EMBS Int. Conf. on Eng. in Medicine and Biology*, 2008, pp. 4575–4578.

[12] G. Venture, K. Ayusawa, and Y. Nakamura, "Dynamics identification of humanoid systems," in *Proc. CISM-IFToMM Symp. on Robot Design, Dynamics, and Control (ROMANSY)*, 2008, pp. 301–308.

[13] Y. Yamaguchi, K. Yamane, and Y. Nakamura, "Identification of muscle, tendon, and mass parameters of musculoskeletal human model," *Proc. of the Conf. on Robotics and Mechatronics*, 2A1-D07, 2006, (in Japanese).

[14] Y. Fujimoto, S. Obata, and A. Kawamura, "Robust biped walking with active interaction control between foot and ground," in *Proc. of the IEEE Int. Conf. on Robotics and Automation*, 1998, p. 2030Ű2035.

[15] K. Yoshida, D.N. Nenchev, and M. Uchiyama, "Moving base robotics and reaction management control," in *Proc. of the Seventh Int. Symp. of Robotics Research*, 1995, p. 100Ű109.

[16] H. Mayeda, K. Osuka, and A. Kangawa, "A new identification method for serial manipulator arms," in *Proc. IFAC 9th World Congress*, 1984, pp. 2429–2434.

[17] C.G. Atkeson, C.H. An, and J.M. Hollerbach, "Estimation of inertial parameters of manipulator loads and lunks," *Int. J. of Robotic Research*, vol. 5, no. 3, pp. 101–119, 1986.

[18] H. Kawasaki, Y. Beniya, and K. Kanzaki, "Minimum dynamics parameters of tree structure robot models," in *Int. Conf. of Industrial Electronics, Control and Instrumentation*, 1991, vol. 2, pp. 1100–1105.

[19] W. Khalil and F. Bennis, "Symbolic calculation of the base inertial parameters of closed-loop robots," *Int. J. of Robotics Research*, vol. 14(2), pp. 112–128, April 1995.

[20] M. Gautier, "Numerical calculation of the base inertial parameters," *J. of Robotic Systems*, vol. 8(4), pp. 485–506, 1991.

[21] K. Ayusawa, G. Venture, and Y. Nakamura, "Inertial parameters identifiability of humanoid robot based on the baselink equation of motion," *Proc. of the Conf. on Robotics and Mechatronics*, 2P1-F09, 2008, (in Japanese).

[22] Y. Nakamura, *Advanced Robotics: Redundancy and Optimization*, Addison-Wesley Longman Publishing Co., Inc, 1990.

[23] M. Mochimaru and M. Kouchi, "Japanese body dimension data," *http://riodb.ibase.aist.go.jp/dhbodydb/97-98/index.html.en*, 1997-98.

[24] J.-J.E.Slotione, W.Li, "Applied Nonlinear Control," *Prentice Hall*, 1991.

[25] M. Gautier and W. Khalil, "Exciting trajectories for the identification of base inertial parameters of robots," *Int. J. of Robotic Research*, vol. 11, no. 4, pp. 363–375, 1992.

[26] G. Venture, K. Ayusawa, and Y. Nakamura, "A numerical method for choosing motions with optimal excitation properties for identification of biped dynamics - an application to human," in *Proc. IEEE Int. Conf. on Robotics and Automation (to be published)*, 2009.

[27] G. Venture, P.J. Ripert, W. Khalil, M. Gautier, and P. Bodson, "Modeling and identification of passenger car dynamics using robotics formalism," *IEEE Trans. on Intelligent Transportation Systems*, vol. 7, no. 3, pp. 349–359, 2006.